Green Chemistry

PAPER

View Article Online
View Journal

Cite this: DOI: 10.1039/d6gc00900j

Process-optimised access to triarylamines through catalytic dehydrogenative aromatisation

Giulia Brufani, †[a] Antonio Vella,†[a] Anastasiia M. Afanasenko, [b] Chao-Jun Li [b] and Luigi Vaccaro *[a]

Received 10th February 2026,
Accepted 26th March 2026

DOI: 10.1039/d6gc00900j

rsc.li/greenchem

Despite growing interest in triarylamines as rapidly advancing materials for optoelectronic and organic photovoltaic applications, their synthesis generally relies on multistep routes and requires functionalization of the starting materials. The development of atom- and step-economical strategies for their preparation remains highly desirable. In parallel, engineering new reaction pathways beyond C–N bond formation *via* cross-coupling is crucial to enhance process sustainability, reduce waste generation and resource consumption, and improve overall system performance. Here, we report the development of a multigram-per-day production Pd-catalysed dehydrogenative aromatisation route to triarylamines, using anilines and potentially lignin-derived cyclohexanones as readily available arylating partners in place of aryl halides. Mild oxidant conditions have been provided by molecular oxygen as the sole oxidant. To enable scale-up while ensuring effective gas–liquid contact, the methodology is implemented in a continuous-flow system comprising multiple packed-bed reactors, where slug flow maintains the aerobic conditions required. Green metrics are assessed against benchmark protocols to contextualise the process within current sustainability frameworks.

Green foundation

1. The growing interest in triarylamines for optoelectronic applications poses significant synthetic challenges. We report a dehydrogenative aromatisation strategy for accessing triarylamines from simple anilines and cyclohexanones, maximising atom and step economy while reducing the *E*-factor, and demonstrating scalability through a continuous-flow process.
2. The green metrics evaluation confirms the substantial improvements of the Pd-catalysed dehydrogenative aromatisation compared to benchmark protocols. The *E*-factors of 5 under flow conditions demonstrates the ability of the developed process to reduce waste generation. Moreover, the increased VMR reflects enhanced human and environmental safety.
3. Future research will focus on the synthesis of triarylamines from lignin-derived phenols and on the exploration of triarylamines as electron donor–acceptor complexes, photoredox catalysts, and functional materials for advanced materials science applications.

Introduction

Characterised by distinctive physicochemical properties, triarylamines are a rapidly growing class of compounds. Due to their distinctive electron-rich architecture, which promotes strong π-conjugation, and their ability to strategically modify aryl substituents to tune electronic properties, triarylamines serve as crucial benchmarks in materials science.[1–3] Their relatively low ionisation potential, lower than that of many organic and inorganic materials, endows them with excellent electron-donating abilities, enabling efficient hole and electron transport.[4–6]

Owing to these characteristics, triarylamine serves as a hole-injecting and hole-transporting layer in OLEDs,[7,8] as an organic sensitiser molecule for solar cells,[9,10] and as a host-emitting material for organic photovoltaic devices.[11,12] It is also employed as a luminescent probe for biomarker detection and environmental sensing,[13,14] and in organic field-effect transistors,[15] nonlinear optical materials, and xerographic applications.[16,17] Additionally, this structural motif shows potential as an effective catalytic donor in light-induced electron donor–acceptor (EDA) complexes for C–H perfluoroalkylation of arenes and heteroarenes,[18] alkylation and cyanation of arenes,[19] visible light sulfonylation reactions,[20] and photoredox complexes.[21]

The synthesis of triarylamines typically relies on a two-step approach, involving the former preparation of diarylamines and their subsequent coupling with aryl halides *via* Cu-promoted

[a]*Laboratory of Green S.O.C. – Dipartimento di Chimica, Biologia e Biotecnologie, Università degli Studi di Perugia, Via Elce di Sotto 8, Perugia 06123, Italy. E-mail: luigi.vaccaro@unipg.it*
[b]*Department of Chemistry, and FQRNT Centre for Green Chemistry and Catalysis, McGill University, 801 Sherbrooke Street West, Montreal, QC H3A0B8, Canada*
†These authors contributed equally.

Ullmann condensation.[22,23] Despite being well established, this methodology typically depends on stoichiometric, or, at best, ligand-assisted catalytic, quantities of Cu(I) or Cu(II) salts, in combination with a large excess of strong inorganic base. Moreover, it generally proceeds under harsh conditions, requiring elevated temperatures (150–220 °C under classical conditions or 80–130 °C in ligand-assisted variants) in polar aprotic solvents such as DMSO, DMF, and NMP. Buchwald–Hartwig coupling is a well-established methodology for accessing triarylamines from diarylamines, catalysed by either homogeneous[24–26] or heterogeneous Pd-based catalysts.[27] Buchwald *et al.* developed a one-pot Pd-catalysed protocol involving the sequential coupling of an aniline with both chloro- and bromoarenes (Fig. 1a).[28] Although these methodologies provide access to a wide variety of symmetrical and unsymmetrical triarylamines with diverse functional groups, they inevitably produce halide salt by-products. This underscores the need for more atom- and step-economical strategies, further developing new reaction pathways beyond the classical "oxidative addition and reductive elimination" mechanism of cross-coupling.[29,30] The transition-metal-catalysed formal cross-coupling of phenols with amines has emerged as an effective strategy for accessing diarylamines, proceeding *via* reduction of the phenol followed by condensation with the amine (Fig. 1b).[31–35]

In recent years, since the pioneering work of Deng and Li in 2012,[36] catalytic dehydrogenative aromatisation has emerged as a means of accessing C–N bonds.[37] This methodology involves a sequence of nucleophilic addition, dehydration, and catalytic oxidative dehydrogenation, employing oxygen as the sole oxidant or hydrogen transfer strategies.[38] Cyclohexanones, which are inexpensive, chemically stable, and readily accessible from lignin-derived biomass, are recognised for their renewable and sustainable character.[39–42] These features make them preferred arylating agents, valuable intermediates in the synthesis of a wide range of industrially prominent compounds.[43,44] They act as efficient arylating agents for synthesising diarylamines from both anilines and nitroarenes, with a Pd-based catalyst facilitating the process (Fig. 1c).[45–50]

Herein, we report a direct, operatively streamlined methodology to access symmetrical triarylamines from anilines and cyclohexanone *via* Pd/C-catalysed oxidative dehydrogenative aromatisation. This method overcomes the challenging requirement of two consecutive condensations between cyclohexanone and anilines, affected by the diminished nucleophilicity of the intermediate diarylamines. Aerobic conditions provide the required oxidative environment, using O_2 as the terminal oxidant and generating water as the sole byproduct (Fig. 1d).[51–54] The process exhibited efficiency in cyclopentyl methyl ether (CPME), a well-established solvent known for its low environmental impact, suitable safety profile, and compatibility under oxidative conditions,[55–57] reflecting the significant influence of the reaction medium on overall environmental sustainability and process efficiency.[58–60]

The development of methodologies beyond traditional oxidative addition–reductive elimination pathways meets the need to establish a process compatible with flow conditions.[61] Conventional approaches typically require overstoichiometric amounts of inorganic bases, which are often insoluble and cause reactor clogging.[27] By avoiding such bases, the proposed strategy ensures efficient mass transport under continuous-flow conditions, thereby improving the safety of O_2 handling.[62,63] This approach enables a multigram-per-day production platform for the synthesis of both diarylamines and triarylamines, while minimising side-product formation, facilitating the recovery of excess reagents, and eliminating the need for labour-intensive and solvent-intensive chromatographic purification. The setup is based on a modular reactor configuration consisting of two packed-bed columns: the first packed with polymer-bound *p*-toluenesulfonic acid (PS-TsOH) and the second loaded with Pd/C. Aerobic oxidation was achieved by introducing gaseous O_2, generating a stable slug-flow regime (Fig. 1d).

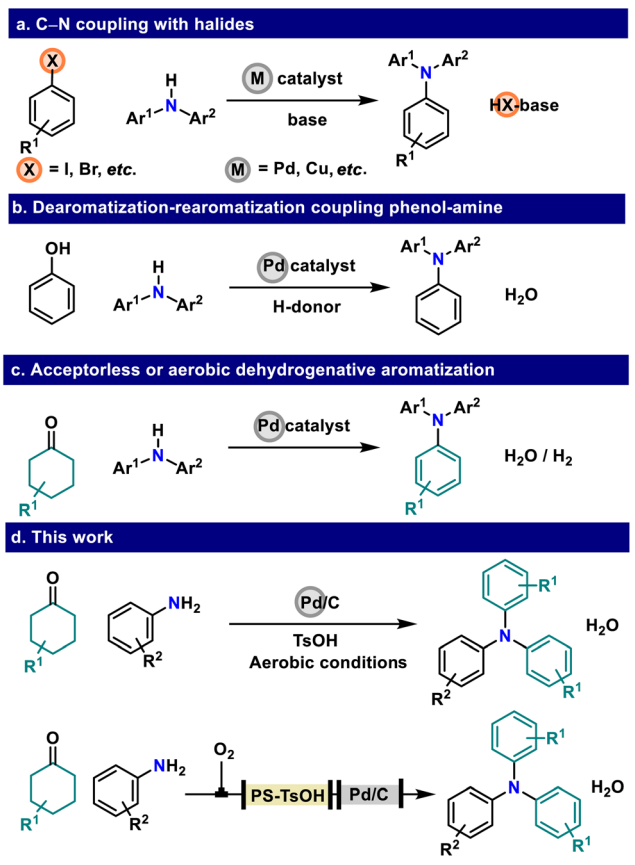

Fig. 1 Overview of synthetic strategies for accessing triarylamines.

Results and discussion

The optimisation of the reaction conditions began with the selection of 4-methylphenylamine (**1a**) and 4-methylcyclohexanone (**2a**) as preferred substrates. Pd/C (10 wt%) was chosen as the heterogeneous catalyst, and TsOH was used as a co-catalyst due to its proven efficiency in promoting dehydrogenative aromatisation.[50] An oxidative aromatic dehydrogenation was performed: the reaction mixture was refluxed in an

open vessel for 16 h, after which O_2 was introduced *via* a balloon (100 mL), so the system remained at atmospheric pressure, and the reaction continued for an additional 6 h.

We began the optimisation by determining the most suitable solvent. Nonpolar aromatic hydrocarbons, such as *p*-xylene, toluene, and mesitylene, exhibited low selectivity toward the desired product **6a**. Specifically, *p*-xylene failed to yield **6a**, instead favouring the formation of intermediate **5a** (Table 1, entry 1). Toluene and mesitylene produced mixtures of **3a** and **4a**, with only trace amounts of **6a** being detected, thereby preventing the second condensation (Table 1, entries 2 and 3). This retention of intermediates is likely attributable to π–π stacking interactions, which stabilise these species within the reaction environment. In contrast, the use of nonpolar ethers, such as 1,4-dioxane, facilitated the second condensation of cyclohexanone, thereby increasing selectivity toward a mixture of **6a** and **5a**. However, this solvent system hindered the complete dehydrogenative aromatisation (Table 1, entry 4). Notably, by employing CPME, complete selectivity for product **6a** was achieved (Table 1, entry 5). It is essential to note that all reactions conducted under these conditions resulted in the complete conversion of the limiting reagent **1a**. A lower concentration of CPME led to decreased conversion, with reagent **1a** remaining partially unreacted, and a mixture of **5a** and **6a** was observed (Table 1, entry 6). Similarly, reducing **2a** from 10 to 5 equiv. led to the formation of both **5a** and **6a** (Table 1, entry 7).

The catalytic amounts of Pd/C and TsOH were optimised to achieve the highest selectivity. Utilising 10 mol% of both Pd/C and TsOH resulted in optimal selectivity toward product **6a**. However, reducing the Pd/C amount from 10 mol% to 2 mol% led to a significant decrease in conversion toward **6a**, favouring the formation of **5a** (Table 1, entries 8 and 9). Notably, performing the reaction with 1 equiv. of TsOH yielded a mixture of **3a** and **5a**, with no formation of the desired product **6a**, thereby preventing the dehydrogenative aromatisation (Table 1, entry 10).

To further elucidate the role of TsOH in the optimised process, additional co-catalyst screening was conducted. TsOH outperformed both CH_3COOH (Table 1, entry 11) and NEt_3 (Table 1, entry 12) in terms of selectivity and yield. Interestingly, the use of polymer-bound TsOH (PS-TsOH) afforded the desired product **6a**, although the dehydrogenative aromatisation of **5a** to **6a** was incomplete (Table 1, entry 13). Furthermore, conducting the reaction without TsOH as a co-catalyst led to incomplete dehydrogenative aromatisation of **5a** to **6a**, even after the addition of O_2 (Table 1, entry 14), underscoring the necessity of TsOH for the desired transformation.

Control experiments without Pd/C yielded no product (Table 1, entries 15 and 16), confirming the catalytic role of Pd in the process.

The reaction was conducted without adding the O_2 balloon after 24 h, resulting in incomplete dehydrogenative aromatisation of **5a** to **6a** (Table 1, entry 17). This outcome highlights the need for an additional oxidising environment. To further support this observation, the reaction was also performed in a screw-capped vial under closed-vessel conditions, confirming the need for O_2 to complete the aromatisation of **5a** (Table 1, entry 18).

With the optimised reaction conditions (Table 1, entry 5) in hand, the substrate scope for the synthesis of symmetric triarylamines was investigated using a range of anilines (**1a–1l**) and cyclohexanones (**2a–2e**). This approach enables 15 triarylamines (**6a–6o**) to be obtained, featuring various functional groups, in moderate to good isolated yields.

Anilines **1a–1d** smoothly afforded the corresponding triarylamines (**6a–6g**). However, the steric hindrance of the aniline and cyclohexanone significantly influenced reactivity. Bulky substituents required prolonged reaction times to achieve full conversion. Replacing the methyl group with more sterically demanding isopropyl (**1e**) or *tert*-butyl (**1f**) groups markedly reduced the reactivity, yielding products **6h–6k** in lower efficiency.

Electronic effects also played a critical role: electron-deficient anilines inhibited product formation. While **1g** furnished triarylamines **6l** and **6m** in moderate yields, anilines **1i** and **1j** remained unreactive under the optimised conditions. In contrast, substrate **1h** successfully delivered products **6n** and **6o** in good yields.

Aniline **1k** underwent dehalogenation, whereas nitro-substituted **1l** yielded a mixture that was difficult to interpret and characterise. Moreover, the bulky 4-*tert*-butylcyclohexanone (**2c**) entirely suppressed product formation, yielding only the

Table 1 Optimisation of the reaction conditions for triarylamine synthesis[a]

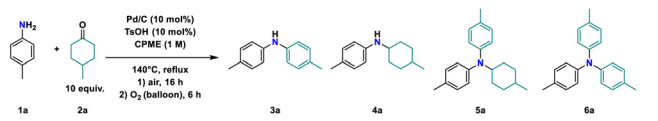

Entry	Reaction medium	Co-catalyst	C[b] (%) 3a	4a	5a	6a
1	*p*-Xylene	TsOH	45	0	55	0
2	Mesitylene	TsOH	50	37	3	10
3	Toluene	TsOH	29	46	9	16
4	1,4-Dioxane	TsOH	9	5	48	38
5	CPME	TsOH	0	0	0	>99
6[c]	CPME	TsOH	0	0	19	56
7[d]	CPME	TsOH	0	0	35	65
8[e]	CPME	TsOH	14	2	42	42
9[f]	CPME	TsOH	44	12	21	24
10[g]	CPME	TsOH	50	0	50	0
11	CPME	AcOH	0	5	75	20
12	CPME	NEt_3	7	0	70	23
13	CPME	PS-TsOH	0	0	40	60
14	CPME	—	0	4	61	35
15[h]	CPME	—	0	0	0	0
16[i]	CPME	TsOH	0	0	0	0
17[j]	CPME	TsOH	6	1	47	46
18[k]	CPME	TsOH	20	7	14	59

[a] Reaction conditions: **1a** (0.5 mmol), **2a** (5 mmol, 10 equiv.), Pd/C (10 wt%, 10 mol%), TsOH (10 mol%), CPME (1 M), reflux, 16 h under air, additional 6 h under a balloon of O_2. [b] Conversion determined by gas–liquid chromatographic analysis; the remaining material is unreacted **1a**. [c] CPME (0.25 M). [d] **2a** (5 equiv.). [e] Pd/C (5 mol%). [f] Pd/C (2 mol%). [g] TsOH (1 equiv.). [h] Standard conditions, no Pd/C and no TsOH. [i] Standard conditions with TsOH and no Pd/C. [j] Open-vessel under reflux, 24 h. [k] Closed vial, 24 h.

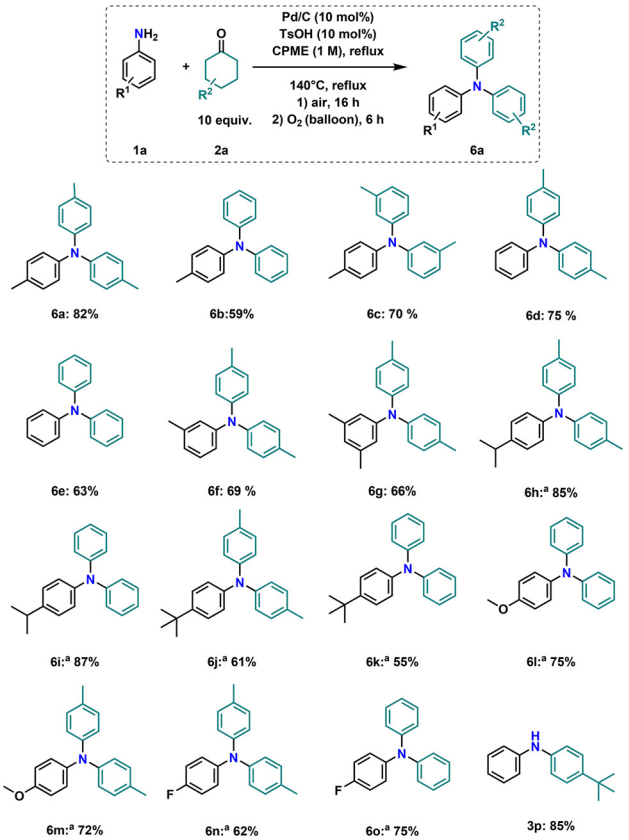

Scheme 1 Scope of symmetric triarylamines. Reaction conditions: **1a** (0.5 mmol), **2a** (5 mmol, 10 equiv), Pd/C (10 mol%), TsOH (10 mol%), CPME (1 M), reflux for 16 h under air, followed by an additional 6 h under an O_2 balloon; [a] reflux for 24 h under air, followed by an additional 24 h under an O_2 balloon.

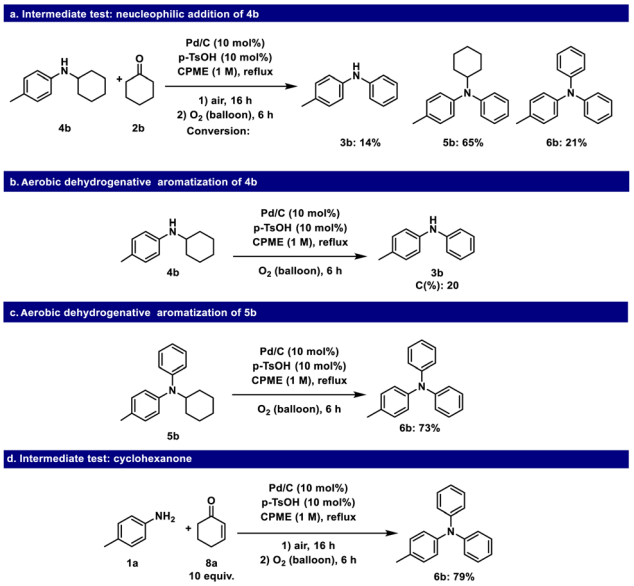

Fig. 2 Control experiment.

intermediate **3p**. Similarly, 2,6-dimethylcyclohexanone (**2d**) proved unreactive, further highlighting the reaction's sensitivity to steric effects (Scheme 1).

At this stage, mechanistic investigations were conducted to elucidate the oxidative dehydrogenative aromatisation pathway under the optimised conditions. The reaction profile was monitored over time to clarify the product distribution. Substrates **1a** and **2a** were rapidly consumed upon initiation, with full conversion into the imine intermediate (7), detected within 5 minutes, which further converted into intermediates **3a** and **4a**, demonstrating that this step is the fastest in the reaction (Fig. S1). The time course for the first minutes of the reaction suggested that **3a** forms primarily *via* the disproportionation of the imine pathway, as this pathway is faster than the dehydrogenative aromatisation of **4a** to **3a**.

In separate experiments, we confirmed that **4b** is active in the reaction pathway leading to diarylamine **3b**, which then undergoes a second arylation to yield the desired triarylamine **6b**. Concurrently, a significant amount of **5b** was produced (Fig. 2a). At this stage, we examined the oxidative dehydrogenative aromatisation of *N*-cyclohexylamine **4b**, promoted by O_2 (*via* a balloon) in CPME at 140 °C for 6 hours. Under these conditions, a reduced amount of just 20% of the desired product **3b** was obtained, confirming that intermediate **4b** preferentially condenses with a second molecule of **2b** instead of undergoing dehydrogenative aromatisation (Fig. 2b).

Due to the excess of **2a**, intermediate **3a** is immediately converted into **6a** and **5a**. This arylation initially favours the formation of **5a** as the major intermediate, which subsequently undergoes dehydrogenative aromatisation to form the final product, **6a**, and then reaches equilibrium. Introducing O_2 *via* a balloon promoted the complete conversion of **5a** into the target product, **6a**, achieving full selectivity within 6 hours (Fig. S1).

We examined the oxidative dehydrogenative aromatisation of *N*-cyclohexyl-4-methyl-*N*-phenylaniline **5b**, promoted by O_2 (*via* a balloon) in CPME at 140 °C for 6 h, obtaining **6b** in an isolated yield of 73% (Fig. 2c). The same experiment performed without Pd/C led to no **6b** formation (Scheme S2). We hypothesise that O_2 guarantees the regeneration of Pd(0) from H–Pd(II)–H, thereby promoting dehydrogenative aromatisation.

To gain further insight into the process, we tested cyclohexen-2-one (**8a**) instead of cyclohexanone. As expected, this resulted exclusively in the formation of product **6b**, as this reagent requires only a single double-bond dehydrogenation to achieve complete aromatisation (Fig. 2d).[64]

Based on the literature, the reaction time course, and control experiments, we propose a plausible reaction mechanism. First, **2** and **1** undergo condensation to form the imine intermediate **7**, which subsequently generates products **3** and **4**. Both intermediates can then undergo a second condensation with an additional molecule of **2**, yielding the target product **6** and the intermediate **5**, which forms an enamine that is barely detectable. The intermediate **5** undergoes Pd-catalysed dehydrogenative aromatisation to form the desired product **6**. The Pd-catalyst plays a crucial role in dehydrogenative aromatisation, while molecular oxygen plays a critical role

in regenerating Pd(0) from the H–Pd–H intermediate, thereby enabling complete selectivity for product **6** (Fig. 3).

The recyclability of Pd/C was investigated. Although the recovered Pd/C catalyst maintained complete conversion of **1a**, a distribution of **3a**, **4a**, **5a**, and the desired product **6a** was obtained (Table S1). To understand the origin of the loss in reactivity, the catalyst was recycled after 16 h of reflux under open-vessel conditions, prior to the addition of the O_2 balloon. Under these conditions, the same ratio between **6a** and **5a** was preserved for two consecutive cycles, but a mixture of **3a**, **4a**, **5a**, and the desired product, **6a**, was obtained in the third run (Table S2).

MP-AES analysis revealed a minimal Pd loss of only 0.1%, confirming that the lack of reactivity was not attributable to Pd leaching into the solution. To assess whether the reaction follows a heterogeneous mechanism, a hot-filtration test was performed after 45 minutes of reaction. Upon removal of the Pd/C catalyst, the reaction stopped, indicating a heterogeneous pathway. This conclusion was further supported by MP-AES analysis at the same stage, which showed Pd loss below 0.1%. The experiment was repeated prior to introducing the O_2 balloon, confirming once again the heterogeneous nature of the reaction (Tables S3 and S4).

STEM analysis of Pd/C, performed before and after the introduction of the O_2 balloon, showed an increase in the nanoparticle size. The average diameter shifted from 2.5–3.5 nm of the fresh Pd/C to 3.5–4.5 nm after 16 h of reaction under atmospheric conditions. In addition, upon introduction of O_2, the fraction of Pd nanoparticles with diameters exceeding 5 nm increased, along with the formation of even larger aggregates. This trend is consistent with the decline in selectivity observed after the first reaction cycle and confirms that O_2 adversely affects the catalyst's recyclability (Fig. 4). Furthermore, EDS and elemental analyses revealed residual traces of sulfur (0.42%) and nitrogen (1.26%), which we hypothesise to contribute to catalyst deactivation.

To address the reduced reactivity of recycled Pd/C, overcome the challenges associated with the use of an unrecoverable and poorly soluble co-catalyst such as TsOH, and facilitate the process scale-up using molecular O_2, we developed a continuous gas–liquid flow system for dehydrogenative aromatisation, employing PS-TsOH as a solid-supported acid co-catalyst.

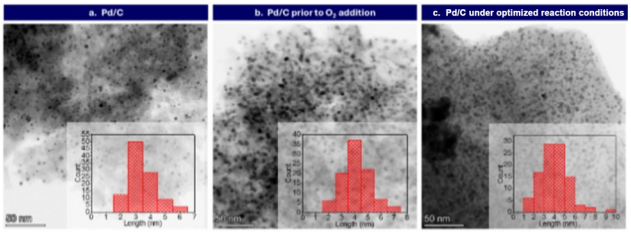

Fig. 4 STEM analysis of (a) fresh Pd/C; (b) Pd/C after 16 h of reaction under atmospheric conditions, prior to the addition of O_2; (c) Pd/C under the optimised reaction conditions.

Substrates **1a** and **2a** were chosen for protocol optimization using a continuous-flow setup comprising two sequential packed-bed reactors: the first packed with 50 mg of PS-TsOH with a commercial loading of 2.5 mmol g^{-1} (R1; length = 4.5 cm; internal diameter = 2 mm) and the second with Pd/C 10 wt% (R2, length = 22 cm; internal diameter = 4 mm). The reaction mixture, consisting of **1a** and **2a** dissolved in CPME, was delivered to R1 *via* an HPLC pump and maintained at room temperature. Gaseous O_2 was introduced into the system *via* a T-junction, and the flow was regulated to maintain a constant slug-flow regime, before it entered R2, which was maintained at 140 °C. An inline back-pressure regulator (BPR) for controlled system pressure was used to maintain a constant pressure inside the apparatus. The outlet stream was collected and analysed by gas–liquid chromatography.

According to the control test, we found that R1 efficiently promotes the condensation of **1a** and **2a**. The continuously produced **7a** then flows directly into R2, where, in the presence of O_2 and Pd/C, it is converted into intermediate **3a**. In contrast, in the absence of gaseous O_2, **7a** is converted into **4a**, which, as observed in the control test under batch conditions, scarcely enables the formation of **3a**. This setup enables tandem condensation and dehydrogenative aromatisation, which is controlled by fine-tuning the reactor length and residence time, thereby enabling the selective synthesis of diarylamine **3a** and triarylamine **6a**. At a flow rate of 0.05 mL min^{-1}, the reaction initially yields a mixture of **7a**, **3a**, and **4a** (Table 2, entry 1). When the equivalent of **2a** is reduced, selectivity shifts away from **3a**, favouring the formation of **4a** (Table 2, entries 2 and 3). A higher dilution and a longer residence time negatively affected the formation of **3a** (Table 2, entry 4). By adjusting the BPR settings, the flow rate was reduced to 0.02 mL min^{-1} and the residence time increased, resulting in the complete formation of product **3a** (Table 2, entry 5). An isolated yield of 92% was achieved (Scheme S1).

To drive the reaction toward **6a**, we increased the reactor length; together with a higher BPR setting, this led to improved conversion (Table 2, entries 6 and 7). Ultimately,

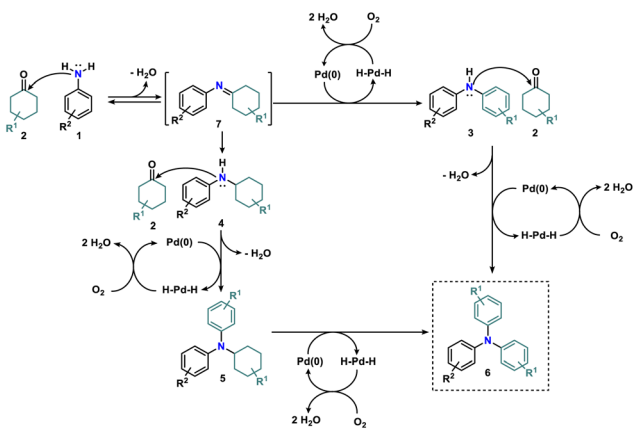

Fig. 3 Proposed reaction mechanism for the synthesis of triarylamines from aniline and cyclohexanone *via* oxidative dehydrogenative aromatisation.

Table 2 Optimisation of the reaction conditions for the selective synthesis of diarylamine and triarylamine under flow[a]

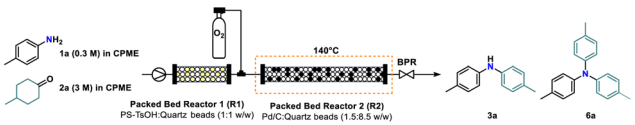

						C[b] (%)				
Entry	Pd (mmol)	R2 (cm)	Flow rate (ml min^{-1})	Residence time (min)	BPR (bar)	**7a**	**3a**	**4a**	**5a**	**6a**
1[c]	0.47	22	0.05	80	2.8	29	39	27	5	0
2[c,d]	0.47	22	0.03	133	2.8	34	52	6	8	0
3[c,e]	0.47	22	0.03	133	2.8	99	0	0	0	0
4	0.47	22	0.03	133	2.8	80	20	0	0	0
5	0.47	22	0.02	200	5.2	0	>99	0	0	0
6c	0.94	44	0.02	400	2.8	0	37	43	5	8
7	0.94	44	0.02	400	5.2	0	47	0	12	41
8	1.41	66	0.02	600	5.2	0	0	0	0	>99

[a] Reaction conditions: **1a** (5 mmol), **2a** (50 mmol, 10 equiv.), and CPME (0.3 M). [b] Conversion determined by gas–liquid chromatographic analysis; the remaining material is unreacted **1a**. [c] CPME (1 M). [d] **2a** (5 equiv.). [e] **2a** (1.5 equiv.).

extending the reactor length enabled complete conversion and maximised **6a** production (Table 2, entry 8).

By optimising the reaction conditions under continuous flow, using an apparatus designed to maximise gas–liquid–solid interactions, the formation of by-products resulting from excess **2a** could be minimised. This result is strategic as, in turn, it opens a route to the purification of compound **6a** without using column chromatography. Therefore, we tested the possibility of isolating the pure products *via* salt precipitation.

After distillation of CPME and recovery of the unreacted **2a** (82%), CPME (5 mL) was added, followed by an aqueous solution of HBF_4 (48 wt%, 1.5 equiv.), leading to formation of the corresponding $[Ar_3NH]^+$ BF_4^- salt as a white precipitate. Precipitation was completed by adding cold heptane, and the resulting solid was collected by filtration. Subsequently, aqueous NaOH (1 M) and the recovered CPME were added. After centrifugation, the distillation of CPME afforded pure **6a** (yield: 88%). The solvents CPME and heptane used in the procedure were recovered by distillation (95% and 92%, respectively) and reused.

The robustness of the flow step-up was tested in the synthesis of **6a**, and for over 83 h of operating time the efficiency was constant, yielding to 89% isolated yield (Scheme S1). The developed system exhibited a space–time yield of 0.181 kg L^{-1} day^{-1}, a TON of 18.5 for Pd/C, and a Pd leachate concentration of 0.4 ppm (Pd loss below 0.1%), indicating the successful synthesis of **6a**.

The green metrics of the developed protocols, evaluated under both batch and flow conditions, were compared with those of representative, well-established methods for obtaining product **6a**. We selected (a) the benchmark Pd-catalysed one-pot synthesis of triarylamines from anilines and two different aryl halides;[28] (b) a Pd-catalysed direct catalytic nitrogenation using N_2 as the nitrogen source;[65] (c) a Pd-catalysed direct catalytic C–N formation employing $NaNH_2$ as the nitrogen source;[66] (d) a heterogeneous N/O-doped carbon-supported nano-Pd catalyst for the synthesis of triarylamines from cyclohexanone and nitrobenzene;[67] (e) a Cu-catalysed C–N coupling reaction for the synthesis of triarylamines from aniline and iodarenes;[68] and (f) an acceptorless dehydrogenative aromatization one-pot triarylamine synthesis from anilines and two different cyclohexanones to achieve the synthesis of first diarylamines and then triarylamines, selecting the product (4-methoxyl-*N*-phenyl-*N*-(*m*-tolyl)aniline), which presented the highest isolated yield for this process.[50] The comparison considered the atom economy (AE), stoichiometric factor (SF), material recovery parameter (MRP), benign index (BI), safety hazard index (SHI), vector magnitude ratio (VMR), reaction mass efficiency (RME), and *E*-factor (Fig. 5; see the SI for detailed calculations and data).

Workup and purification steps were explicitly included in the green assessment. Heterogeneous catalytic systems were assumed to be fully recovered from the reaction mixture. The amounts of materials used for chromatographic purifications were, in all cases, considered identical, considering the eluent being recoverable by distillation for all procedures. Additionally, solvents were considered recoverable by distillation only if used in volumes larger than 10 mL.

The use of 4-methylcyclohexanone as an arylating agent significantly improves the AE compared to well-established protocols that rely on bromo- and chloroarenes as starting materials, making this method comparable to that reported by Yamaguchi *et al.* (Fig. 5).[50]

Despite the lack of LD_{50} and LC_{50} data for some starting materials, evaluation of the safety hazard index (SHI) and benign index (BI) indicates that the major contribution arises from solvent selection and dilution, while the reactants themselves have a more moderate impact. In particular, the use of toluene and 1,4-dioxane at low concentrations negatively affects these metrics. However, this effect is partially mitigated when toluene is used at higher concentrations, as in the protocol reported by Buchwald *et al.* (Fig. 5; see the SI for SHI and BI calculations using different starting materials).

Our protocols exhibit high BI and SHI values, particularly under flow conditions, approaching 0.95 (optimal case = 1).

Regarding the benchmark processes analysed, the use of inorganic bases necessitates additional aqueous extraction steps.

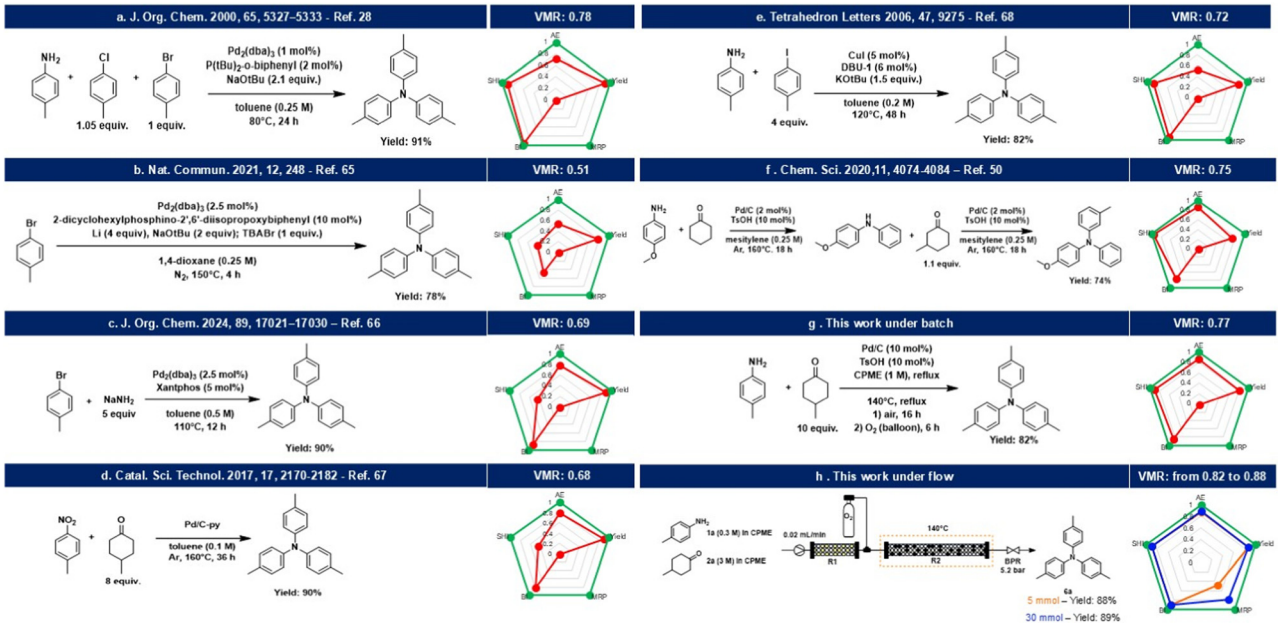

Fig. 5 Green metrics evaluation and comparison of the developed methodology under batch and flow conditions with benchmark methodologies.

The presence of homogeneous Pd catalysts, excess reagents, and incomplete conversion to triarylamines requires purification of the targeted product by column chromatography. Similarly, the batch protocol reported herein suffers from the use of excess cyclohexanones, leading to by-product formation and necessitating chromatographic purification, thereby increasing waste production as reflected by a high *E*-factor and a low RME. *E*-Factor profiles confirmed that the highest impact on waste generation occurs in the purification step (Fig. 6).

On the other hand, the flow setup enables efficient control over reaction selectivity, thereby minimising side-product formation and facilitating the recovery of the reagents used in excess. It should be noticed that selectivity towards the triarylamine is crucial for its successful purification. In fact, the presence of partially aromatised products formed in the absence of oxygen makes the purification tedious and sometimes impossible even by column chromatography, due to the very similar natures of all the possible products. In these cases, only theoretical yields could be reported. The presence of oxygen allows high selectivity towards the product and, therefore, satisfactory actual isolation yields.

We also proved that it is also possible to eliminate the chromatographic purification by forming the corresponding BF_4^- salt. This is relevant at a larger scale that is achievable using the optimised flow protocol, which also leads to a significant improvement in the mass-based green metrics (MRP, RME, and the *E*-factor).

In fact, pure product isolation was achieved through a carefully optimised salification–precipitation protocol, in which the amounts of acid and anti-solvent were tuned to ensure quantitative precipitation of the target compound while minimising inorganic waste generation in the aqueous phase. This strategy limits waste formation primarily to aqueous streams and inorganic salts. As a result, the *E*-factor is reduced from values above 100 to 5.3 and 4.8 for the transformation of 5 mmol and 3 mmol of **1a** to **6a**, respectively (Fig. 6).

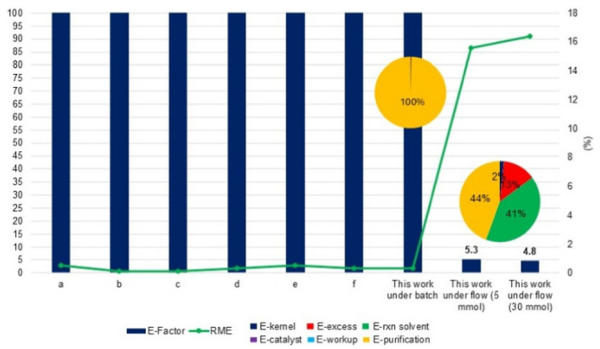

Fig. 6 Comparison of the *E*-factor and RME for the developed methodology under batch and flow conditions *versus* benchmark processes, including *E*-factor contribution analysis.

Experimental section

General procedure for the synthesis of triarylamines

In a 10 mL round-bottom flask equipped with a magnetic stirrer, Pd/C (10 mol%; 53 mg), TsOH (10 mol%; 8.6 mg), CPME (1 M; 0.5 mL), 1 (0.5 mmol), and 2 (5 mmol, 10 equiv.) were consecutively added. The reaction was stirred at 140 °C in an open vessel under reflux for 16 hours. Then, an O_2 balloon was connected to the apparatus, and the reaction was stirred for an additional 6 hours at 140 °C. Pd/C was filtered from the reaction mixture and washed with CPME (10 mL). The pure

product was obtained by column chromatography on silica with ETP as the eluent.

General procedure for the synthesis under flow

Setup 1: *p*-toluidine (**1a**) (5 mmol, 530 mg) and 4-methylcyclohexanone (**2a**) (50 mmol, 10 equiv., 6 mL) were dissolved in CPME (16.7 mL, 0.3 mol L^{-1}). PS-TsOH (50 mg, 2.5 mmol g^{-1}) was mixed with 1 mm glass beads in a 1 : 1 ratio and packed into a 4.5 cm stainless steel reactor with an internal diameter of 2 mm (R1). The Pd/C 10 wt% (0.47 mmol of Pd) was mixed with 1 mm-diameter glass beads in a 1.5 : 8.5 ratio and packed into a 22 cm stainless steel reactor with an internal diameter of 4 mm (R2). R1 was placed at room temperature. R2 was placed at 140 °C. Both reactors were placed in a laboratory-made continuous-flow system equipped with a T-junction to introduce gaseous O_2 (0.25 mL min^{-1}) upstream of R2, thereby establishing a slug-flow regime. The entire system was equipped with a 5.2 bar BPR. The solution of **1a** and **2a** in CPME was delivered to the system *via* an HPLC pump at an effective flow rate of 0.02 mL min^{-1}. After a residence time of 200 min, complete conversion into **3a** was achieved. After distillation of CPME and recovery of the unreacted **2a** (82%), CPME (5 mL) was added, followed by an aqueous solution of HBF_4 (48 wt%, 1.5 equiv.). Precipitation was completed by adding cold heptane (5 mL), and the resulting solid was collected by filtration.

Subsequently, aqueous NaOH (3 M, 2 mL) and the recovered CPME (5 mL) were added. After centrifugation, the distillation of CPME afforded pure **3a** (yield: 92%). The solvents CPME and heptane used in the procedure were recovered by distillation (95% and 92%, respectively) and reused.

Setup 2: *p*-toluidine (**1a**) (5 mmol, 530 mg) and 4-methylcyclohexanone (**2a**) (50 mmol, 10 equiv., 6 mL) were dissolved in CPME (16.7 mL, 0.3 mol L^{-1}). PS-TsOH (50 mg, 2.5 mmol g^{-1}) was mixed with 2 mm glass beads in a 1 : 1 ratio and packed into a 4.5 cm stainless steel reactor with an internal diameter of 2 mm (R1). Pd/C 10 wt% (1.41 mmol of Pd) was mixed with 2 mm-diameter glass beads in a 1.5 : 8.5 ratio and packed into a 66 cm stainless steel reactor with an internal diameter of 4 mm (R2). R1 was placed at room temperature. R2 is placed at 140 °C. Both reactors were placed in a laboratory-made continuous-flow system, equipped with a T-junction to introduce the gaseous O_2 (0.25 mL min^{-1}) upstream of R2, thereby establishing a slug-flow regime. The entire system was equipped with a 5.2 bar BPR. The solution of **1a** and **2a** in CPME was delivered to the system *via* an HPLC pump at an effective flow rate of 0.02 mL min^{-1}. After a residence time of 600 min, complete conversion to **6a** was achieved. The conversion was evaluated by gas chromatographic analysis.

After distillation of CPME and recovery of the unreacted **2a** (82%), CPME (5 mL) was added, followed by an aqueous solution of HBF_4 (48 wt%, 1.5 equiv.). Precipitation was completed by adding cold heptane (5 mL), and the resulting solid was collected by filtration.

Subsequently, aqueous NaOH (3 M, 2 mL) and the recovered CPME (5 mL) were added. After centrifugation, the distillation of CPME afforded pure **6a** (yield: 88%). The solvents CPME and heptane used in the procedure were recovered by distillation (95% and 92%, respectively) and reused.

Conclusions

In conclusion, we developed a practical and scalable strategy for direct access to triarylamines *via* Pd/C-catalysed oxidative dehydrogenative aromatisation, using anilines and potentially lignin-derived cyclohexanones as readily accessible arylating partners, in both batch and continuous-flow systems. The optimised conditions were applied to the synthesis of 15 variously functionalized symmetric triarylamines.

The protocols rely on Pd/C as a heterogeneous metal-based catalyst and TsOH as a co-catalyst. After rapid condensation, products **3** and **4** were formed. Both intermediates could then undergo a second condensation with an additional molecule of **2**, yielding the target product **6** and the intermediate **5**, which can be fully converted into **6**. The Pd-catalyst plays a crucial role in dehydrogenative aromatisation. O_2 serves as the sole oxidant, playing the crucial role of regenerating Pd(0) from H–Pd–H, thereby enabling complete selectivity for the target product.

An increase in Pd nanoparticle aggregation led to a progressive decline in catalytic activity over successive runs.

To address the reduced reactivity of recycled Pd/C, overcome the challenges associated with using an unrecoverable, poorly soluble co-catalyst, such as TsOH, and facilitate process scale-up using molecular O_2, a continuous gas–liquid flow system was developed. This system employed multiple column reactors packed with Pd/C and PS-TsOH as a solid-supported acid co-catalyst. The system operates under slug flow with gaseous O_2, maintaining aerobic conditions while improving efficiency and robustness.

The robustness of the flow step-up was tested through an 83-hour synthesis, representative of the synthesis of **6a**, achieving an isolated yield of 89%. The developed system exhibited a space–time yield of 0.181 kg L^{-1} day^{-1}, a TON for Pd/C of 18.5, and a Pd leaching of 0.4 ppm.

Finally, the developed continuous-flow methodology enables enhanced control of the selectivity of the reaction. This aspect is crucial as it allows the actual isolation of the pure products without tedious and sometimes impossible column chromatography purifications, minimises by-product formation, and allows efficient recovery of excess reagents. The elimination of chromatographic purification, achieved through an optimized salification–precipitation protocol, significantly reduces solvent consumption and waste generation. As a result, the process shows a marked improvement in VMR, and the *E*-factor decreases from values above 100 to 5.

Author contributions

The manuscript was written through the contributions of all authors. All authors have given approval to the final version of the manuscript.

Conflicts of interest

There are no conflicts to declare.

Data availability

The data supporting this article have been included as part of the supplementary information (SI). Supplementary information is available. See DOI: https://doi.org/10.1039/d6gc00900j.

Acknowledgements

This publication was prepared with the support and funding from the European Union – NextGenerationEU under the Italian Ministry of University and Research (MUR) National Innovation Ecosystem grant ECS00000041 – VITALITY. MUR is thanked for the PRIN-2022 project "20223ARWAY – REWIND". This work was supported by the funding from the Canada Research Chair Foundation, the FQRNT Center for Green Chemistry and Catalysis, the National Science and Engineering Research Center (NSERC), and McGill University. A. F. thanks FQRNT for a postdoctoral fellowship. Zeon Corporation, Japan, is acknowledged for kindly supporting our work with free samples of CPME.

References

1 B.-B. Cui, Y. Han, N. Yang, S. Yang, L. Zhang, Y. Wang, Y. Jia, L. Zhao, Q.-Y. Zhong and Y.-W. Chen, *ACS Appl. Mater. Interfaces*, 2018, **10**, 41592–41598.
2 E. Moulin, J. J. Armao and N. Giuseppone, *Acc. Chem. Res.*, 2019, **52**, 975–983.
3 Q.-M. Koh, N. S. Mazlan, Q.-J. Seah, J.-C. Yang, Y.-J. Chen, R.-Q. Png, P. K. H. Ho and L.-L. Chua, *ACS Appl. Mater. Interfaces*, 2024, **16**, 39708–39716.
4 R. Fuentes Pineda, Y. Zems, J. Troughton, M. R. Niazi, D. F. Perepichka, T. Watson and N. Robertson, *Sustainable Energy Fuels*, 2020, **4**, 779–787.
5 P. Cias, C. Slugovc and G. Gescheidt, *J. Phys. Chem. A*, 2011, **115**, 14519–14525.
6 R. A. Klenkler and G. Voloshin, *J. Phys. Chem. C*, 2011, **115**, 16777–16781.
7 M. Thelakkat, *Macromol. Mater. Eng.*, 2002, **287**, 442.
8 S. Jhulki and J. N. Moorthy, *J. Mater. Chem. C*, 2018, **6**, 8280–8325.
9 J. Wang, K. Liu, L. Ma and X. Zhan, *Chem. Rev.*, 2016, **116**, 14675–14725.
10 D. Devadiga, M. Selvakumar, P. Shetty, M. Santosh, R. S. Chandrabose and S. Karazhanov, *Int. J. Energy Res.*, 2021, **45**, 6584–6643.
11 Z. Ning and H. Tian, *Chem. Commun.*, 2009, **37**, 5483.
12 Y.-H. Cheng, H.-L. Wong, E. Y.-H. Hong, S.-L. Lai, M.-Y. Chan and V. W.-W. Yam, *ACS Appl. Energy Mater.*, 2020, **3**, 3059–3070.
13 Y.-D. Deng, Q. Liu, D. Wang, Z.-W. Pan, T.-T. Du, Z.-X. Yuan and W.-J. Yi, *Bioorg. Chem.*, 2024, **152**, 107742.
14 S. Ravi, S. Karthikeyan, M. Pannipara, A. G. Al-Sehemi, D. Moon and S. P. Anthony, *Spectrochim. Acta, Part A*, 2024, **319**, 124557.
15 R. Dheepika, A. Shaji, P. M. Imran and S. Nagarajan, *Org. Electron.*, 2020, **81**, 105568.
16 Z. Mei, Y. Zhang, S. Sun, Y. He and H. Meng, *Chem. Eng. J.*, 2025, **526**, 171341.
17 L. Huang, R. Guo, Q. Qiu, H. Li, P. Balla, J. Zeng, T. Liang, X. Qi and P. Liu, *Chem. Eng. J.*, 2024, **497**, 155018.
18 D. J. Castillo-Pazos, J. D. Lasso, E. Hamzehpoor, J. Ramos-Sánchez, J. M. Salgado, G. Cosa, D. F. Perepichka and C.-J. Li, *Chem. Sci.*, 2023, **14**, 3470–3481.
19 A. Dewanji, L. van Dalsen, J. A. Rossi-Ashton, E. Gasson, G. E. M. Crisenza and D. J. Procter, *Nat. Chem.*, 2023, **15**, 43–52.
20 J. D. Lasso, D. J. Castillo-Pazos, J. M. Salgado, C. Ruchlin, L. Lefebvre, D. Farajat, D. F. Perepichka and C.-J. Li, *J. Am. Chem. Soc.*, 2024, **146**, 2583–2592.
21 J. Schütte, D. Corsi, W. Haumer, S. Schmid, J. Žurauskas and J. P. Barham, *Green Chem.*, 2024, **26**, 6446–6453.
22 J. H. Gorvin, *J. Chem. Soc., Perkin Trans. 1*, 1988, 1331.
23 H. B. Goodbrand and N.-X. Hu, *J. Org. Chem.*, 1999, **64**, 670–674.
24 J. F. Hartwig, M. Kawatsura, S. I. Hauck, K. H. Shaughnessy and L. M. Alcazar-Roman, *J. Org. Chem.*, 1999, **64**, 5575–5580.
25 T. Kanbara, K. Izumi, T. Narise and K. Hasegawa, *Polym. J.*, 1998, **30**, 66–68.
26 M. A. Topchiy, P. B. Dzhevakov, M. S. Rubina, O. S. Morozov, A. F. Asachenko and M. S. Nechaev, *Eur. J. Org. Chem.*, 2016, 1908–1914.
27 G. Brufani, S. Chen, M. T. Tiberi, F. Campana, E. Paone, Y. Gu, F. Mauriello and L. Vaccaro, *Green Chem.*, 2025, **27**, 3869–3878.
28 M. C. Harris and S. L. Buchwald, *J. Org. Chem.*, 2000, **65**, 5327–5333.
29 Z. Qiu, H. Zeng and C.-J. Li, *Acc. Chem. Res.*, 2020, **53**, 2395–2413.
30 Z. Qiu and C.-J. Li, *Chem. Rev.*, 2020, **120**, 10454–10515.
31 Z. Chen, H. Zeng, S. A. Girard, F. Wang, N. Chen and C.-J. Li, *Angew. Chem.*, 2015, **127**, 14695–14699.
32 T. Cuypers, P. Tomkins and D. E. De Vos, *Catal. Sci. Technol.*, 2018, **8**, 2519–2523.
33 K. Chen, Q.-K. Kang, Y. Li, W.-Q. Wu, H. Zhu and H. Shi, *J. Am. Chem. Soc.*, 2022, **144**, 1144–1151.
34 Z. Chen, H. Zeng, H. Gong, H. Wang and C.-J. Li, *Chem. Sci.*, 2015, **6**, 4174–4178.
35 M. Ortega, B. Garrido, D. Gómez, A. A. Fernandez-Andrade, M. E. Domine, R. Jiménez and L. E. Arteaga-Pérez, *ChemCatChem*, 2025, **17**, 2.
36 S. A. Girard, X. Hu, T. Knauber, F. Zhou, M.-O. Simon, G.-J. Deng and C.-J. Li, *Org. Lett.*, 2012, **14**, 5606–5609.

37 T. Matsuyama, T. Yatabe, T. Yabe and K. Yamaguchi, *Nat. Commun.*, 2025, **16**, 1118.
38 S. A. Girard, H. Huang, F. Zhou, G.-J. Deng and C.-J. Li, *Org. Chem. Front.*, 2015, **2**, 279–287.
39 X. Zhang, T. Wang, L. Ma, Q. Zhang, X. Huang and Y. Yu, *Appl. Energy*, 2013, **112**, 533–538.
40 J. Zhang, X. Kuang, L. Zhu, X. Xiao, Z. Zhou and F. Qi, *Fuel*, 2025, **383**, 133863.
41 L. Wang, X. Cheng, M. Dong, S. Luan, Y. Wu, B. Han and H. Liu, *Chem. Res. Chin. Univ.*, 2024, **40**, 29–35.
42 K. Wang, Z. Li, Z. Guo, J. Huang, T. Liu, M. Zhou, J. Hu and H. Li, *Green Chem.*, 2024, **26**, 2454–2475.
43 X. Liu, J. Chen and T. Ma, *Org. Biomol. Chem.*, 2018, **16**, 8662–8676.
44 K. Deng, H. Huang and G.-J. Deng, *Org. Biomol. Chem.*, 2021, **19**, 6380–6391.
45 Y. Xie, S. Liu, Y. Liu, Y. Wen and G.-J. Deng, *Org. Lett.*, 2012, **14**, 1692–1695.
46 K. Taniguchi, X. Jin, K. Yamaguchi, K. Nozaki and N. Mizuno, *Chem. Sci.*, 2017, **8**, 2131–2142.
47 A. Hajra, Y. Wei and N. Yoshikai, *Org. Lett.*, 2012, **14**, 5488–5491.
48 L. E. Arteaga-Pérez, R. Manrique, F. Castillo-Puchi, M. Ortega, C. Bertiola, A. Pérez and R. Jiménez, *Chem. Eng. J.*, 2021, **417**, 129236.
49 Y. Zeng, B. Wang, Y. Li, X. Yan, L. Chen and Y. Wang, *Ind. Eng. Chem. Res.*, 2020, **59**, 1436–1445.
50 S. Takayama, T. Yatabe, Y. Koizumi, X. Jin, K. Nozaki and K. Yamaguchi, *Chem. Sci.*, 2020, **11**, 4074–4084.
51 F. Chen, H. Geng, C. Li, J. Wang, B. Guo, L. Tang and Y.-Y. Yang, *J. Org. Chem.*, 2023, **88**, 15589–15596.
52 W.-C. Lin, T. Yatabe and K. Yamaguchi, *Chem. Lett.*, 2025, **54**, 3.
53 S. Sharma, F. Gallou and S. Handa, *Green Chem.*, 2024, **26**, 6289–6317.
54 D. Prat, A. Wells, J. Hayler, H. Sneddon, C. R. McElroy, S. Abou-Shehadad and P. J. Dunn, *Green Chem.*, 2016, **18**, 288–296.
55 G. de Gonzalo, A. R. Alcántara and P. Domínguez de María, *ChemSusChem*, 2019, **12**, 2083–2097.
56 U. Azzena, M. Carraro, L. Pisano, S. Monticelli, R. Bartolotta and V. Pace, *ChemSusChem*, 2019, **12**, 40–70.
57 K. Watanabe, N. Yamagiwa and Y. Torisawa, *Org. Process Res. Dev.*, 2007, **11**, 251–258.
58 V. Hessel, N. N. Tran, M. R. Asrami, Q. D. Tran, N. Van Duc Long, M. Escribà-Gelonch, J. O. Tejada, S. Linke and K. Sundmacher, *Green Chem.*, 2022, **24**, 410–437.
59 G. Quaglia, F. Campana, L. Latterini and L. Vaccaro, *ACS Sustainable Chem. Eng.*, 2022, **10**, 9123–9130.
60 K. Watanabe, *Molecules*, 2013, **18**, 3183–3194.
61 T. Ichitsuka, I. Takahashi, N. Koumura, K. Sato and S. Kobayashi, *Angew. Chem.*, 2020, **132**, 16025–16030.
62 C. A. Hone and C. O. Kappe, *Top. Curr. Chem.*, 2019, **377**, 2.
63 C. A. Hone, D. M. Roberge and C. O. Kappe, *ChemSusChem*, 2017, **10**, 32–41.
64 A. Dominguez-Huerta, I. Perepichka and C.-J. Li, *ChemSusChem*, 2019, **12**, 2999–3002.
65 K. Wang, Z.-H. Deng, S.-J. Xie, D.-D. Zhai, H.-Y. Fang and Z.-J. Shi, *Nat. Commun.*, 2021, **12**, 248.
66 C. Sivarajan, S. Saha, S. Mulla and R. Mitra, *J. Org. Chem.*, 2024, **89**, 17021–17030.
67 S. Pang, Y. Zhang, Y. Huang, H. Yuan and F. Shi, *Catal. Sci. Technol.*, 2017, **7**, 2170–2182.
68 Y.-H. Liu, C. Chen and L.-M. Yang, *Tetrahedron Lett.*, 2006, **47**, 9275.

